

Resonant spin-dependent electron coupling in a III-V/II-VI heterovalent double quantum well

A. A. Toropov, I. V. Sedova, S. V. Sorokin, Ya. V. Terent'ev, E. L. Ivchenko, and S. V. Ivanov

Ioffe Physico-Technical Institute, Russian Academy of Sciences, St. Petersburg 194021, Russia

(Received 4 February 2005; published 11 May 2005)

We report on design, fabrication, and magneto-optical studies of a III-V/II-VI hybrid structure containing a GaAs/AlGaAs/ZnSe/ZnCdMnSe double quantum well (QW). The structure design allows one to tune the QW levels into the resonance, thus facilitating penetration of the electron wave function from the diluted magnetic semiconductor ZnCdMnSe QW into the nonmagnetic GaAs QW, and *vice versa*. Magneto-photoluminescence studies demonstrate level anticrossing and strong intermixing resulting in a drastic renormalization of the electron effective g factor, in perfect agreement with the energy level calculations.

DOI: 10.1103/PhysRevB.71.195312

PACS number(s): 78.67.Pt, 85.75.Mm, 75.50.Pp, 75.70.Cn

I. INTRODUCTION

The great majority of currently used semiconductor device heterostructures are *isovalent*, i.e., they involve compounds of the same chemical group. The design and fabrication of *heterovalent* heterostructures, including compounds of different groups, are hampered because of the lack of precise data on the properties and technology of heterovalent interfaces. Particularly discouraging are the charge accumulation at the interfaces and poor technological reproducibility of such basic interface properties as band offsets which depend on the detail of the atomic structure and composition of the interface.¹⁻³ On the other hand, certain useful characteristics of the heterovalent structures are unachievable in the isovalent ones. One known example is the reduced hole leakage in mid-infrared optoelectronic devices based on InAs, due to the realization of a huge valence band offset (VBO) at an InAs/CdSe interface.⁴

Another opportunity can be a flexible engineering of magneto-electronic and magneto-optical properties in a III-V/II-VI hybrid quantum structure allowing a coherent coupling of electrons confined in a III-V part, e.g., a GaAs/AlGaAs quantum well (QW), and a diluted magnetic semiconductor (DMS) II-VI part, e.g. a ZnCdMnSe/ZnSe QW. Such structures can combine the magnetically tunable spin-dependent electron confining potential in the II-VI DMS part,⁵ and high electron mobilities as well as long electron spin relaxation times in a non-magnetic III-V part.⁶ This combination can be useful for both fundamental studies of spin-polarized two-dimensional electron gas and device applications in the rapidly growing field of spintronics. Note that the magnetic tuning of spin-dependent electron coupling was previously observed in spin superlattices^{7,8} and double QWs⁹ consisting of diluted magnetic and nonmagnetic II-VI semiconductors. However, to the best of our knowledge, the electron resonant coupling through a heterovalent interface has never been observed.

Realization of the proposed design relies on the controlled fabrication of a high-quality interface between the III-V and II-VI parts. The (Al)GaAs/ZnSe interface is at present most studied among other heterovalent interfaces.^{3,10-12} Its technology was thoroughly developed for the growth of ZnSe-based optoelectronic devices on GaAs substrates.^{13,14} More

recently, the injection of spin-polarized electrons through a GaAs/ZnSe heterointerface has been realized in an (In)GaAs/AlGaAs QW light-emitting diode with a II-VI DMS spin aligner grown on top.^{15,16} Furthermore, photoluminescence was detected from an AlAs/GaAs/ZnSe QW with a heterovalent interface.¹⁷

In this paper we report on the realization of a double QW structure, where a GaAs/AlGaAs QW is electronically coupled with a DMS ZnCdMnSe/ZnSe QW through a heterovalent AlGaAs/ZnSe interface. We show that the proper structure design allows one to achieve resonant tunnelling conditions, which facilitates an extension of the electron wave function in the II-VI DMS region, resulting in giant values of the effective g factor in both the GaAs-like and ZnCdMnSe-like electronic states.

The paper is organized as follows. In Sec. II we describe the design and functionality of the heterovalent double QW structure and present the calculations of electron levels in an external magnetic field. Furthermore, the variational method is briefly outlined, which allows one to calculate excitonic states in the electronically coupled QWs. In Sec. III the sample growth and magnetic-field-dependent photoluminescence (PL) measurements are introduced. Based on the fitting of the energies of circularly polarized excitonic emission peaks, we discuss resonant properties of the heterovalent coupled QWs.

II. THEORETICAL BACKGROUND

The sample design and principles of operation are illustrated in Fig. 1. Figure 1(a) shows schematically the conduction band lineup of the proposed structure. The QW parameters are chosen in such a way that at zero magnetic field the lowest confined electron level in the ZnCdMnSe QW is nearly resonant with the lowest electron level in the GaAs QW. The calculated squared envelope wave function of the lowest-energy electron state in the coupled QWs at zero magnetic field is plotted in Fig. 1(b) (solid curve). The electron probability is distributed between the two QWs. The primary effect of a relatively low external magnetic field applied in the Faraday geometry is a giant Zeeman splitting in the DMS QW, caused by the exchange interaction between electrons and Mn²⁺ ions.⁵ As a result, the magnetic field

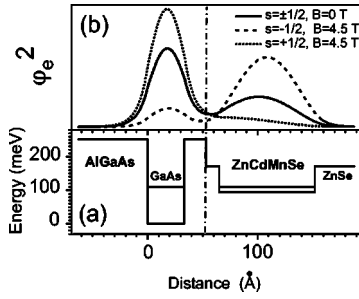


FIG. 1. (a) Conduction band lineup of the double QW sample. Geometrical parameters correspond to the experimental sample with the 3.4-nm-wide GaAs QW. (b) Spin-up (dotted curve) and spin-down (dashed curve) squared electron wave functions calculated for the magnetic field 4.5 T. A solid curve shows the zero-field wave function.

removes spin degeneracy, pushing the electron level with spin component $s=-1/2$ down and the level $s=+1/2$ up. Due to the splitting, the interwell coupling strength is different for the electrons with different spin orientations. The spin asymmetry is well seen in Fig. 1(b) showing the ground state electron wave functions for $s=\pm 1/2$ at the magnetic field $B=4.5$ T. The calculation is performed by using the envelope function approach as well as the mean-field approximation while describing Brillouin-like paramagnetic behavior of the Mn^{2+} ions.⁵

The calculated electron levels versus magnetic field are shown in Fig. 2. The diamagnetic shift of the levels as well as the Zeeman level splitting due to the intrinsic g factors are neglected since they are weak as compared with the effect of exchange interaction with the magnetic ions. The dashed and dotted curves in Fig. 2 illustrate the variation of energy levels in the corresponding uncoupled single QWs. Within the used approximation the level in the isolated GaAs QW remains spin degenerate (dashed curve). At zero magnetic field, due to the interwell coupling, the levels are repulsed, but the double degeneracy is not lifted. As the field increases, the single-QW levels with $s=-1/2$ first approach each other,

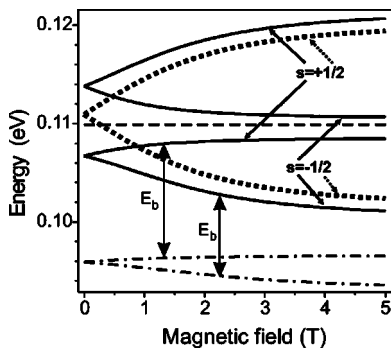


FIG. 2. Electron level variation with the magnetic field in the double QW structure. The structure parameters are the same as in Fig. 1. Dashed and dotted curves represent the levels in isolated GaAs and ZnCdMnSe QWs, respectively. Solid curves show the four levels in the coupled QWs, while a pair of dash-and-dotted curves shows the lowest spin-up and spin-down electron levels with subtracted exciton binding energies.

merge at $B \approx 0.3$ T and then move apart. This explains a drastic anticrossing of these levels when the interwell coupling is switched on. In contrast, the increasing magnetic field loosens the interwell coupling of the levels with $s=1/2$. This resonant magnetic-field-induced control of level mixing should manifest itself in magneto-optical spectra not only in a giant splitting between the lowest levels with $s=\pm 1/2$ but also in a remarkable red-shift of their center of mass. Penetration of the heavy hole states into the ZnCdMnSe QW is prohibited due to the huge valence band offset at the GaAs/ZnSe interface (~ 1.1 eV) as well as the larger value of the effective mass.

While calculating the exciton energies we used the self-consistent variational method and chose factorized exciton envelope functions similar to the procedure applied in Ref. 18. The probe exciton envelope function was taken in the form

$$\Psi = \varphi_e(z_e) \varphi_h(z_h) f(\rho), \quad (1)$$

where $\varphi_e(z)$ and $\varphi_h(z)$ are the single-particle electron and hole envelope functions, the envelope function $f(\rho)$ describes the in-plane electron-hole relative motion, z is directed along the growth direction, and ρ denotes the electron-hole in-plane distance. The hole envelope φ_h is fixed due to strong confinement in the GaAs QW, its dependence on the magnetic field can be ignored. The electron envelope function is more flexible, and it can be redistributed, as compared with a single-electron state, between the two coupled QWs due to the electron-hole Coulomb attraction. The self-consistent solution of the coupled Schrödinger equations for the envelopes $\varphi_e(z)$ and $f(\rho)$ was found numerically. The relevance of this procedure for the description of the experimental spectra of excitonic emission is discussed in the next section.

III. EXPERIMENTAL RESULTS AND DISCUSSION

The samples were grown by molecular-beam epitaxy on GaAs(001), with the III-V and II-VI growth chambers being connected via an ultrahigh vacuum transfer module. The GaAs QW sandwiched between $\text{Al}_{0.3}\text{Ga}_{0.7}\text{As}$ barriers was grown at a substrate temperature $T_S=580$ °C and a low As/III flux ratio, just sufficient to provide $(2 \times 4)\text{As}$ reconstruction during the growth of AlGaAs layers. The top barrier was as thin as 2 nm. It was capped by one monolayer of GaAs to prevent contamination of the AlGaAs surface in the transfer chamber. The grown AlGaAs/GaAs QW structure was cooled down with the $(2 \times 4)\text{As}$ reconstruction. Thereafter the structure was transferred to the II-VI chamber where it was heated up to 280 °C keeping the $(2 \times 4)\text{As}$ reconstruction unchanged. The II-VI growth was initiated under the surface exposure to Se flux, as short as necessary to change the $(2 \times 4)\text{As}$ surface reconstruction to a (2×1) pattern. The latter was stable during the following 30-seconds-long exposure to Zn flux. According to this procedure, one could expect the formation of a Zn-rich interface with a slight admixture of selenium. The ZnSe growth occurred under the $(2 \times 1)\text{Se}$ -stabilized surface conditions. The II-VI part contained a $\text{Zn}_{0.87}\text{Cd}_{0.08}\text{Mn}_{0.05}\text{Se}$ 9-nm-wide QW embedded be-

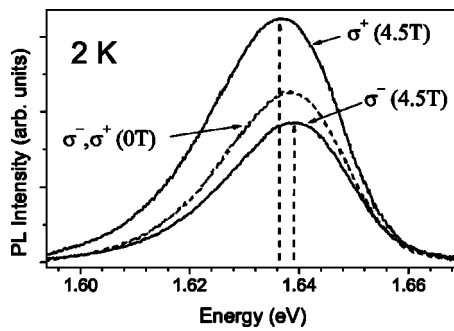


FIG. 3. σ^+ and σ^- polarized PL spectra measured at 0 T (dashed curves) and 4.5 T (solid curves) in the sample with a 3.4 nm wide GaAs QW.

tween 1.2- and 20-nm-thick ZnSe barriers on bottom and top, respectively.

The thickness of the combined AlGaAs/ZnSe barrier between the GaAs and ZnCdMnSe QWs totals 3.2 nm. The AlGaAs layer is inserted in order to move the heterovalent interface with presumably enhanced density of defects aback from the GaAs QW. The ZnSe spacer is needed for proper II-VI growth initiation and for preventing Mn diffusion in the III-V part, since even low content of Mn in III-V compounds damages their optical quality. The total barrier thickness governs the transfer integral between the single-QW electron wave functions and, hence, the strength of the interwell coupling.

Furthermore, reference samples were grown, containing either an additional isolated GaAs QW placed in the bulk of the $\text{Al}_{0.3}\text{Ga}_{0.7}\text{As}$ layer ~ 15 nm apart from the heterovalent interface, or an isolated $\text{Zn}_{0.87}\text{Cd}_{0.08}\text{Mn}_{0.05}\text{Se}$ QW separated from the heterovalent interface by a 20-nm-thick ZnSe buffer.

A saturation value of the Zeeman splitting for electrons confined within the ZnCdMnSe QW lies in the range of 15–20 meV. This means that the zero-field interlevel energy spacing should be preset to within 10 meV. The fulfillment of this requirement is complicated by the drastic dependence of the conduction band offset (CBO) at a GaAs/ZnSe interface on growth conditions. When the interface growth regime changes from Zn-rich to Se-rich, CBO has been found to vary from 100 meV to 600 meV.³ We fixed the interface growth conditions, as described above, and grew a set of structures with a different width of the GaAs QWs, which was controlled by growth rate calibrations and transmission electron microscopy measurements. Most intriguing results have been obtained in the double-QW structure with a 3.4-nm-thick GaAs QW.

To study the effects of interwell electronic coupling we have measured low-temperature spectra of GaAs QW excitonic photoluminescence (PL) in a magnetic field applied in the Faraday geometry. A linearly polarized emission of the 514 nm line of an Ar^+ laser was used as an excitation source. Figure 3 shows the PL spectra of circularly polarized emission components measured in the sample with a 3.4-nm-wide GaAs QW at 0 T (dashed curves) and 4.5 T (solid curves). The PL linewidth amounts to 26 meV and does not depend on the magnetic field. This value is nearly two times more

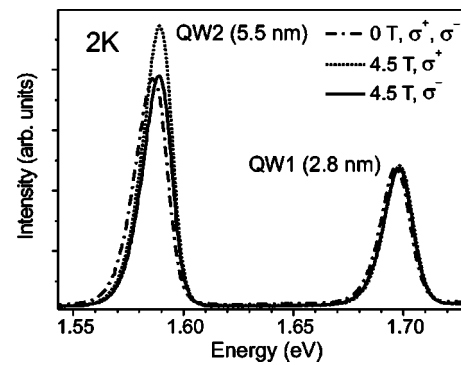


FIG. 4. Circularly polarized PL spectra measured at 0 T (dash-and-dotted curve) and 4.5 T (solid and dotted curves) in the reference sample with an isolated GaAs QW (QW1) and off-resonant double-QW (QW2).

than the change of exciton energy, corresponding to a single-monolayer variation of the QW width, which implies the presence of some broadening mechanism that is more efficient than the broadening due to lateral monomolecular fluctuations of the QW width. To elucidate this point we have measured PL spectra in the sample containing a 2.8-nm-wide reference GaAs QW (QW1) placed in the bulk of the AlGaAs barrier, in addition to a 5.5-nm-wide GaAs QW (QW2) separated by the 3.2-nm-wide barrier with a heterovalent interface from a 9-nm-wide ZnCdMnSe QW. Figure 4 shows the PL spectrum measured in this sample at 0 T (dash-dotted curve) as well as σ^+ (dotted curve) and σ^- (solid curve) spectra measured at 4.5 T. The spectrum consists of two excitonic emission lines of comparable intensity, corresponding to these two QWs. For the reference QW1 the linewidth amounts to 14 meV that is comparable with the energy of the respective single-monolayer fluctuation of the QW width (~ 17 meV). This confirms dominance of the conventional line-broadening mechanism caused by the well width fluctuations.

For the QW2 located only 2 nm apart from the AlGaAs/ZnSe heterovalent interface, the PL linewidth is 16 meV, which is nearly threefold more than the calculated energy variation caused by the single-monolayer thickness fluctuation of the 5.5-nm-wide QW (~ 6 meV). Therefore we assume that the vicinity of the heterointerface results in some additional inhomogeneous broadening of the QW exciton, originating most probably from the fluctuating electric field induced by interface dipoles. Then the even stronger PL line broadening observed in the double-QW sample with the more narrow 3.4-nm-wide QW reflects the deeper penetration of the electron wave function into the QW barrier and, hence, the enhanced sensitivity to the interface disorder. Nevertheless, one should note that the QW2 PL line position fits reasonably well the energy expected for the 5.5-nm-wide QW at zero electric field, which indicates a weakness of the average electric field induced by the heterovalent interface at the position of the QW2.

To determine the energy positions of the relatively wide PL peaks a polynomial was fitted to the data points, following the approach suggested in Ref. 19. The statistical uncertainty limiting the measurement accuracy was estimated as

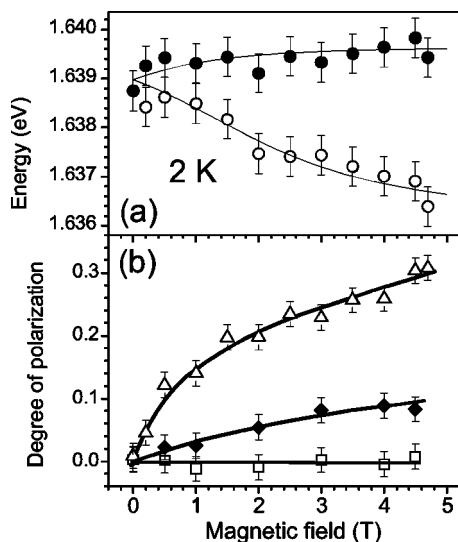


FIG. 5. (a) Energy of the PL peaks corresponding to $| -1/2, 3/2 \rangle$ (open circles) and $| 1/2, -3/2 \rangle$ (solid circles) excitons, measured as a function of the magnetic field. Solid lines represent a theoretical fit (see the text). (b) Degree of σ^+ circular polarization of PL, measured in a resonant double-QW (open triangles), off-resonant double-QW (solid diamonds), and isolated GaAs QW (open squares). Solid curves are drawn only to guide the eye.

± 0.4 meV. No splitting between σ^\pm polarized PL lines was observed for the QW1 and QW2 excitons in the covered range of magnetic fields below 4.5 T (see Fig. 4). According to the optical selection rules, the emission components σ^+ and σ^- are due to the radiative recombination of the dipole-active excitons $| -1/2, 3/2 \rangle$ and $| 1/2, -3/2 \rangle$, respectively. Here we use the notation $| s, m \rangle$ for an exciton with the electron spin $s = \pm 1/2$ and the hole angular momentum component $m = \pm 3/2$. In the conventional GaAs/AlGaAs QWs the exciton splitting is determined by the electron and hole intrinsic g factors. Both of them are very small, so that the respective splitting at 4.5 T does not exceed 0.3 meV for any reasonable QW width.¹⁹ These values are within the experimental error that explains the unobservable splitting of the PL line corresponding to the reference isolated QW (QW1).

On the other hand, the PL spectral peaks in the double-QW sample with the 3.4-nm-wide QW are split at 4.5 T by ~ 3 meV, the lowest-energy peak being σ^+ polarized (see Fig. 3). The peak energy positions are plotted in Fig. 5(a) as a function of the magnetic field. These dependencies reflect neither the Zeeman splitting expected for a conventional GaAs/AlGaAs QW nor the symmetrical giant splitting typical for a single DMS QW. Indeed, for a single 3.4-nm GaAs-based QW, the expected spin splitting at 4.5 T would be as small as ~ 0.3 meV, taking into account the values $g_e \sim 0.1$ and $g_{hh} \sim -1.6$ for the electron and heavy-hole g factors.¹⁹ Moreover, according to the signs of g_e and g_{hh} , the lowest-energy exciton should be $| 1/2, -3/2 \rangle$, which is active in the σ^- polarization. The experimentally observed ordering of the spin-split excitons is opposite. On the other hand, the observed spin splitting between the $| -1/2, 3/2 \rangle$ and $| 1/2, -3/2 \rangle$ exciton states is quite asymmetric, namely, the exciton level $| 1/2, -3/2 \rangle$ is rather stable so that the main

part of the magnetic-field-induced splitting is contributed by a red shift of the $| -1/2, 3/2 \rangle$ exciton level. Therefore we can unambiguously attribute the character of the observed PL band splitting to the effect of resonant coupling between electronic states in the nonmagnetic and DMS QWs. This interpretation explains the fact that no remarkable splitting has been observed in the double-QW sample with the thicker GaAs QW (QW2). The electron level in this 5.5-nm-wide QW lies 45 meV below the electron level in the 3.4-nm-wide QW. Therefore the electronic levels in the nonmagnetic and magnetic QWs are remote far enough to prevent a remarkable effect of interwell coupling on the exciton energy.

To describe the experimental data quantitatively, we have calculated the spin-dependent energies of $| 1/2, -3/2 \rangle$ and $| -1/2, 3/2 \rangle$ excitons as a function of magnetic field in the coupled QW system. The conventional parameters were taken for the GaAs and AlGaAs band gaps, effective masses and band offsets.²⁰ The permittivity $\epsilon = 11$ was used as an average between those of GaAs ($\epsilon \approx 13$) and ZnSe ($\epsilon \approx 9$). To fix the parameters of the ZnCdMnSe/ZnSe QW we have measured the spectra of excitonic reflection in an external magnetic field in a reference isolated ZnCdMnSe QW grown under the same conditions as the DMS QW in the double-QW samples. The lowest-energy σ^+ polarized $| -1/2, 3/2 \rangle$ exciton is well visible in the whole range of magnetic fields, confirming the type I band offsets at the ZnCdMnSe/ZnSe interface. The performed theoretical fit of the exciton energy versus magnetic field has allowed us to obtain the effective Mn concentration $x_{\text{eff}} = 0.03$ and value 1.84 K of the parameter T_0 , describing antiferromagnetic coupling between the Mn^{2+} ions.⁵ For the s - d and p - d exchange integrals, we took the values $N_0\alpha = 0.26$ and $N_0\beta = -1.31$, as in pure ZnMnSe.²¹ Assuming that 75% of the total band offset at the ZnCdMnSe/ZnSe interface falls on the conduction band, the conduction and valence band offsets were obtained as 76 meV and 25 meV, respectively. The relatively small VBO implies that the upper σ^- polarized $| 1/2, -3/2 \rangle$ exciton becomes a type II exciton at ~ 1.5 T. However, the CBO is large enough to ensure the symmetric splitting of the electrons with $s = \pm 1/2$, as shown in Fig. 2 by the dotted lines.

To compare the theory with the PL experimental data, the Stokes shift adopted as $0.6\Delta_{\text{PL}}$, Δ_{PL} being the full width at half maximum of the PL peak,²² was subtracted from the calculated free-exciton energy. CBO at the GaAs/ZnSe interface was considered as the only fitting parameter, while CBO at the AlGaAs/ZnSe interface was calculated assuming the validity of the transitivity rule for ZnSe/GaAs and ZnSe/AlAs heterojunctions.¹² The best theoretical fit shown in Fig. 5(a) by solid lines was obtained in that way, assuming the GaAs/ZnSe CBO to be equal to 171 meV. This value corresponds to a “mixed” Zn-rich interface,³ in agreement with the short surface exposure to Se at the initial stage of the II-VI growth. Note that this procedure was performed intentionally to bring the QW levels into a resonance in a structure with suitable QW widths.

As mentioned in Sec. II, the self-consistent calculation procedure takes into account the redistribution of the electron wave function between the two coupled QWs due to the electron-hole Coulomb attraction. The relevance of this ap-

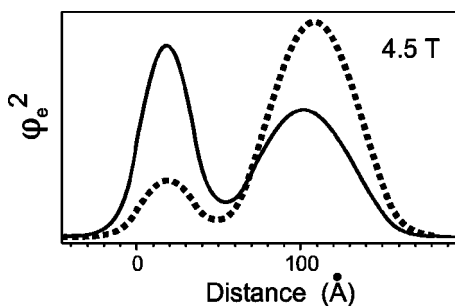


FIG. 6. Electron density $\phi_e^2(z)$ for the spin-down lowest-energy electron state calculated at 4.5 T either neglecting (dotted curve) or taking into account (solid curve) the Coulomb-attraction-induced redistribution of the electron envelope function.

proach is illustrated in Fig. 6 showing the shape of ϕ_e^2 at 4.5 T, calculated either self-consistently (solid curve) or neglecting the Coulomb-attraction-induced redistribution of the electron probability (dotted curve). The Coulomb attraction results in a remarkable increase of probability to find the electron in the GaAs QW. As a consequence, the self-consistent exciton binding energy increases by about 30%.

To illustrate the effect of electron-hole Coulomb interaction on the exciton spin splitting we depicted in Fig. 2, by a pair of dash-and-dotted curves, the spin-up and spin-down lowest-energy electron levels reduced by the self-consistent exciton binding energy. Since the hole energy is independent of the magnetic field, the difference between the curves gives the actual exciton splitting. In agreement with the above analysis the spin-up exciton level is only weakly dependent on the magnetic field. The self-consistent spin-down level approaches, at high magnetic fields, the indirect exciton formed by an electron confined within the ZnCdMnSe QW and a hole confined within the GaAs QW. It is important to stress that, in comparison with the direct (intrawell) exciton, the indirect exciton is characterized by the weaker electron-hole Coulomb interaction and smaller binding energy. The latter effect tends to reduce the exciton spin splitting as compared with the spin splitting of the single-electron levels. In particular, at 4.5 T the exciton spin splitting of 3 meV corresponds to the single-electron spin splitting of 7.2 meV. The difference would be even larger if the calculation did not take into account the Coulomb induced redistribution of electron probability and the pronounced difference between the electron effective masses in GaAs ($0.067m_0$) and ZnCdMnSe ($\sim 0.16m_0$).

In the performed analysis we have neglected diamagnetic shifts both in III-V and II-VI parts of the structure. This approximation is reliably justified for the wide-bandgap QW based on ZnSe, where the diamagnetic shift was estimated as $3\text{--}4 \mu\text{eV}/\text{T}^2$.²³ In the GaAs QWs the diamagnetic shift is about ten times larger, decreasing in the limit of narrow QWs.²⁴ From the spectra shown in Fig. 4 one can deduce that at 4.5 T the diamagnetic shift amounts to ~ 2.5 meV in the 5.5-nm-wide QW and to ~ 1 meV in the 2.8-nm-wide QW. The extrapolation of these data for a 3.4-nm-wide isolated GaAs QW gives the value ~ 1.3 meV. In the double-QW structure near the resonance the diamagnetic shift should be reduced due to the high probability to find

electrons in the II-VI part. At 4.5 T this probability is larger for the spin-down electron level that can result in certain overestimation of the spin splitting, if the diamagnetic shift is not taken into account. However, we believe that this correction is of the order of the experimental inaccuracy and can result only in an insignificant underestimation of the GaAs/ZnSe CBO as obtained from the fitting procedure.

Figure 5(b) shows the degree of σ^+ circular polarization of PL, measured as a function of the magnetic field in the resonant double-QW with the 3.4-nm-wide GaAs QW, off-resonant double-QW with the 5.5-nm-wide GaAs QW (QW2), and reference 2.8-nm-wide isolated QW (QW1). The polarization degree is defined as $(I^{\sigma^+} - I^{\sigma^-}) / (I^{\sigma^+} + I^{\sigma^-})$, where I^{σ^+} and I^{σ^-} are the integrated intensities of the respective PL components. The PL of the isolated QW is practically unpolarized. Since the linearly polarized light excites equal populations of σ^+ and σ^- active excitons, it means that the spin splitting is smaller than the thermal energy $k_B T$ and/or the spin relaxation is ineffective. The emission of the off-resonant double-QW (QW2) is weakly σ^+ polarized, so that the polarization degree at 4.5 T amounts to 0.1. According to Ref. 19 the lowest allowed spin-split exciton in an isolated 5.5-nm-wide GaAs/AlGaAs QW is the σ^- polarized $|1/2, -3/2\rangle$ exciton. The change of the polarization sign indicates the penetration of the electron wave function in the DMS QW even in the off-resonant sample, while the effect is weak and the respective splitting could not be resolved.

The spin splitting in the resonant double-QW at 4.5 T is much larger than $k_B T$ which is $\sim 170 \mu\text{eV}$ at 2 K. Nevertheless the polarization degree at 4.5 T is as small as 0.3. This immediately indicates that the exciton spin lifetime is comparable to the radiative recombination time. The latter can hardly be much less than the lifetime of localized excitons in the conventional III-V or II-VI type I QWs, which usually falls within a 100–400 ps range. Such a low rate of exciton spin relaxation might look surprising for the DMS structures, where the carrier spins suffer from an efficient spin-flip exchange with the magnetic ions.^{25,26} One should note, however, that exciton spin dynamics in DMS was found to be rather complicated and sample-dependent due to an interplay of various factors. Besides the strong $sp-d$ exchange interactions the spin dynamics is governed by the electron-hole exchange interaction,^{27,28} mixing of valence bands,^{29–31} and exciton localization.^{32,33} In particular, remarkably long spin relaxation time of the order of 1 ns was demonstrated for localized excitons in strained ZnMnSe epilayers.³¹ Strong dependence of the degree of circular polarization of excitonic emission on spin splitting was observed in ZnMnSe-based spin superlattices.³⁰ For the spin splitting value 3 meV the polarization degree was ~ 0.4 , which is comparable to the polarization degree 0.3 obtained in our resonant double-QW sample at the same spin splitting. In view of these data the observed rather slow exciton spin relaxation rate does not appear impossible. Time resolved measurements of exciton spin dynamics are necessary to clarify this point.

IV. CONCLUSIONS

In conclusion, we have demonstrated resonant electronic coupling through a heterovalent AlGaAs/ZnSe interface in

an optical-quality double QW with the DMS II-VI part. The structure design allows one to resonantly enhance penetration of the nonmagnetic QW electron wave function into the DMS region and enhance the QW electron g factor by more than one order of magnitude. Such structures are especially beneficial for exciton optical studies, since the electron wave function at resonance has a minimum (see the dashed curve in Fig. 1(b)) at the heterovalent interface with a presumably large density of defects and electrical dipoles, which otherwise could mess up the excitonic properties. However, even in the double-QW structure the presence of the heterovalent interface manifests itself in an additional inhomogeneous broadening of excitons. Therefore the exciton linewidth and energy in the double-QW structures of this type can be con-

sidered as a sensitive indicator of both interface quality and strength of the electric fields induced by the heterovalent interface. Another potential advantage of these hybrid DMS structures is a possibility to insert a similar double QW in a p - i - n or Schottky diode, allowing thus an electric control over the electron spin polarization.

ACKNOWLEDGMENTS

This work was supported by the Program of the PS department of RAS, INTAS (01-2375), VW Foundation and RFBR (02-02-17643, 03-02-17566). S. V. I. is grateful to RSSF.

-
- ¹W. A. Harrison, E. A. Kraut, J. R. Waldrop, and R. W. Grant, *Phys. Rev. B* **18**, 4402 (1978).
- ²R. M. Martin, *J. Vac. Sci. Technol.* **17**, 978 (1980).
- ³R. Nicolini, L. Vanzetti, G. Mula, G. Bratina, L. Sorba, A. Franciosi, M. Peressi, S. Baroni, R. Resta, A. Baldereschi, J. E. Angelo, and W. W. Gerberich, *Phys. Rev. Lett.* **72**, 294 (1994).
- ⁴S. V. Ivanov, V. A. Kaygorodov, S. V. Sorokin, B. Ya. Meltser, V. A. Solovev, Ya. V. Terent'ev, O. G. Lyublinskaya, K. D. Moiseev, E. A. Grebenshchikova, M. P. Mikhailova, A. A. Toropov, Yu. P. Yakovlev, P. S. Kop'ev and Zh. I. Alferov, *Appl. Phys. Lett.* **82**, 3782 (2003).
- ⁵J. K. Furdyna, *J. Appl. Phys.* **64**, R29 (1988).
- ⁶J. M. Kikkawa and D. D. Awschalom, *Phys. Rev. Lett.* **80**, 4313 (1998).
- ⁷M. von Ortenberg, *Phys. Rev. Lett.* **49**, 1041 (1982).
- ⁸N. Dai, H. Luo, F. C. Zhang, N. Samarth, M. Dobrowolska, and J. K. Furdyna, *Phys. Rev. Lett.* **67**, 3824 (1991).
- ⁹D. A. Tulchinsky, J. J. Baumberg, D. D. Awschalom, N. Samarth, H. Luo, and J. K. Furdyna, *Phys. Rev. B* **50**, 10 851 (1994).
- ¹⁰G. Bratina, L. Vanzetti, L. Sorba, G. Biasiol, A. Franciosi, M. Peressi, and S. Baroni, *Phys. Rev. B* **50**, 11 723 (1994).
- ¹¹A. Kley and J. Neugebauer, *Phys. Rev. B* **50**, 8616 (1994).
- ¹²S. Rubini, E. Milocco L. Sorba, A. Franciosi, *J. Cryst. Growth* **184/185**, 178 (1998).
- ¹³M. A. Haase, J. Qiu, J. M. DePuydt, and H. Cheng, *Appl. Phys. Lett.* **59**, 1272 (1991).
- ¹⁴E. Kato, H. Noguchi, M. Nagai, H. Okuyama, S. Kijima, and A. Ishibashi, *Electron. Lett.* **34**, 282 (1998).
- ¹⁵R. Fiederling, M. Keim, G. Reuscher, W. Ossau, G. Schmidt, A. Waag, and L. W. Molenkamp, *Nature (London)* **402**, 787 (1999).
- ¹⁶B. T. Jonker, Y. D. Park, B. R. Bennett, H. D. Cheong, G. Ki-oseoglou, and A. Petrou, *Phys. Rev. B* **62**, 8180 (2000).
- ¹⁷A. Kudelski, U. Bindley, J. K. Furdyna, M. Dobrowolska, and T. Wojtowicz, *Appl. Phys. Lett.* **82**, 1854 (2003).
- ¹⁸E. L. Ivchenko, A. V. Kavokin, V. P. Kochereshko, G. R. Posina, I. N. Uraltsev, D. R. Yakovlev, R. N. Bicknell-Tassius, A. Waag, and G. Landwehr, *Phys. Rev. B* **46**, 7713 (1992).
- ¹⁹M. J. Snelling, E. Blackwood, C. J. McDonagh, R. T. Harley, and C. T. B. Foxon, *Phys. Rev. B* **45**, R3922 (1992).
- ²⁰I. Vurgaftman, J. R. Meyer, and L. R. Ram-Mohan, *J. Appl. Phys.* **89**, 5815 (2001).
- ²¹A. Twardowski, M. von Ortenberg, M. Demianiuk, and R. Pauthenet, *Solid State Commun.* **51**, 849 (1984).
- ²²K. P. O'Donnel, P. J. Parbrook, F. Yang, and C. Trager-Cowan, *Physica B* **191**, 45 (1993).
- ²³J. Puls, V. V. Rossin, F. Henneberger, and R. Zimmermann, *Phys. Rev. B* **54**, 4974 (1996).
- ²⁴H. Okamoto, *Jpn. J. Appl. Phys., Part 1* **26**, 315 (1987).
- ²⁵G. Bastard and L. L. Chang, *Phys. Rev. B* **41**, R7899 (1990).
- ²⁶R. Ferreira and G. Bastard, *Phys. Rev. B* **43**, 9687 (1991).
- ²⁷M. Z. Maialle, E. A. de Andrada e Silva, and L. J. Sham, *Phys. Rev. B* **47**, 15 776 (1993).
- ²⁸M. R. Freeman, D. D. Awschalom, J. M. Hong, and L. L. Chang, *Phys. Rev. Lett.* **64**, 2430 (1990).
- ²⁹T. Uenoyama and L. J. Sham, *Phys. Rev. Lett.* **64**, 3070 (1990).
- ³⁰W. C. Chou, A. Petrou, J. Warnock, and B. T. Jonker, *Phys. Rev. B* **46**, R4316 (1992).
- ³¹C. D. Poweleit, A. R. Hodges, T.-B. Sun, L. M. Smith, and B. T. Jonker, *Phys. Rev. B* **59**, 7610 (1999).
- ³²H. Nickolaus, H.-J. Wünsche, and F. Henneberger, *Phys. Rev. Lett.* **81**, 2586 (1998).
- ³³M. Z. Maialle, *Phys. Rev. B* **61**, 10 877 (2000).